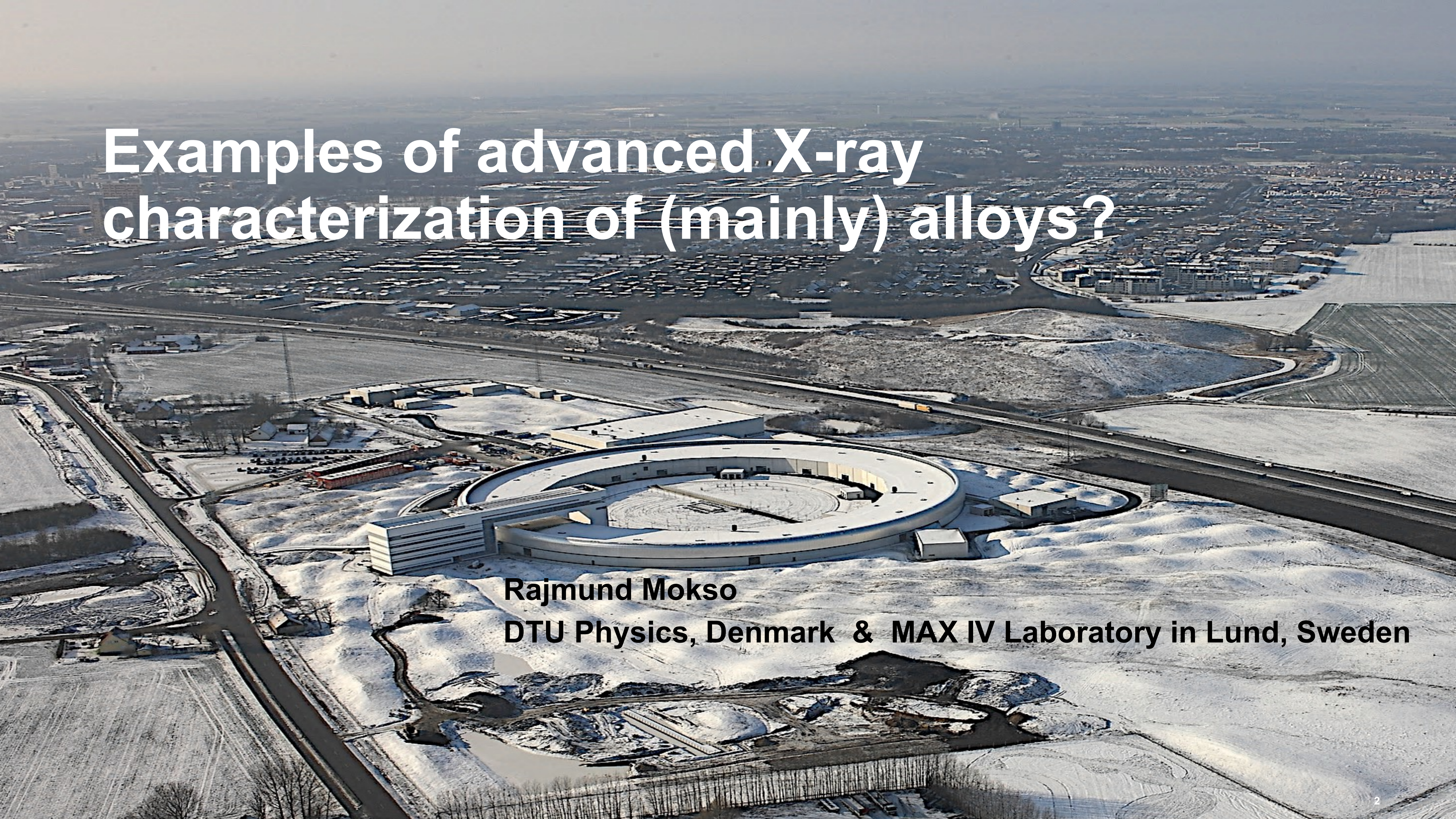

Examples of advanced X-ray characterization of (mainly) alloys?

Rajmund Mokso
DTU Physics, Denmark & MAX IV Laboratory in Lund, Sweden

Imaging methods with 3D capabilities

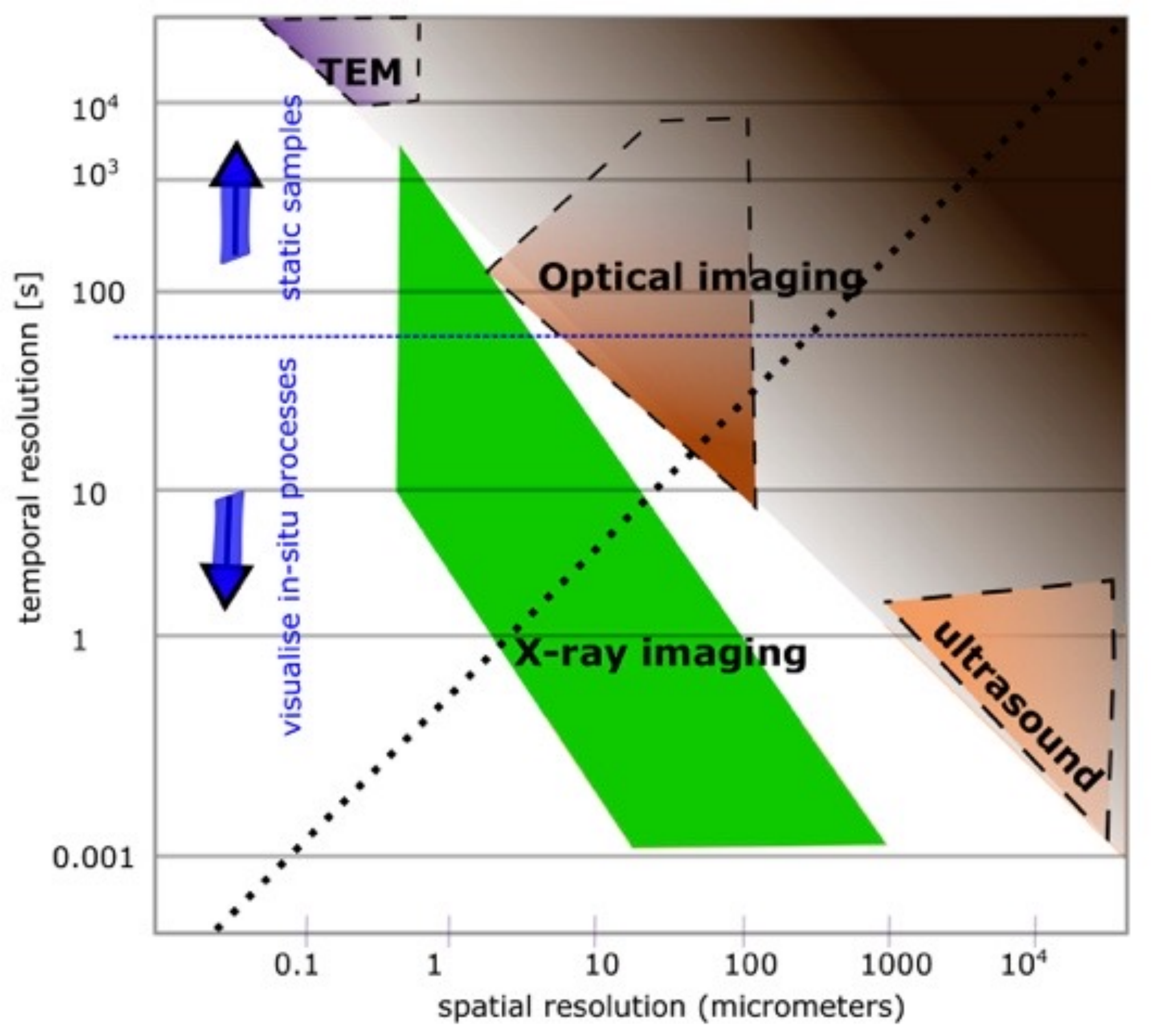

Fast tomography: in-situ visualization of fracture

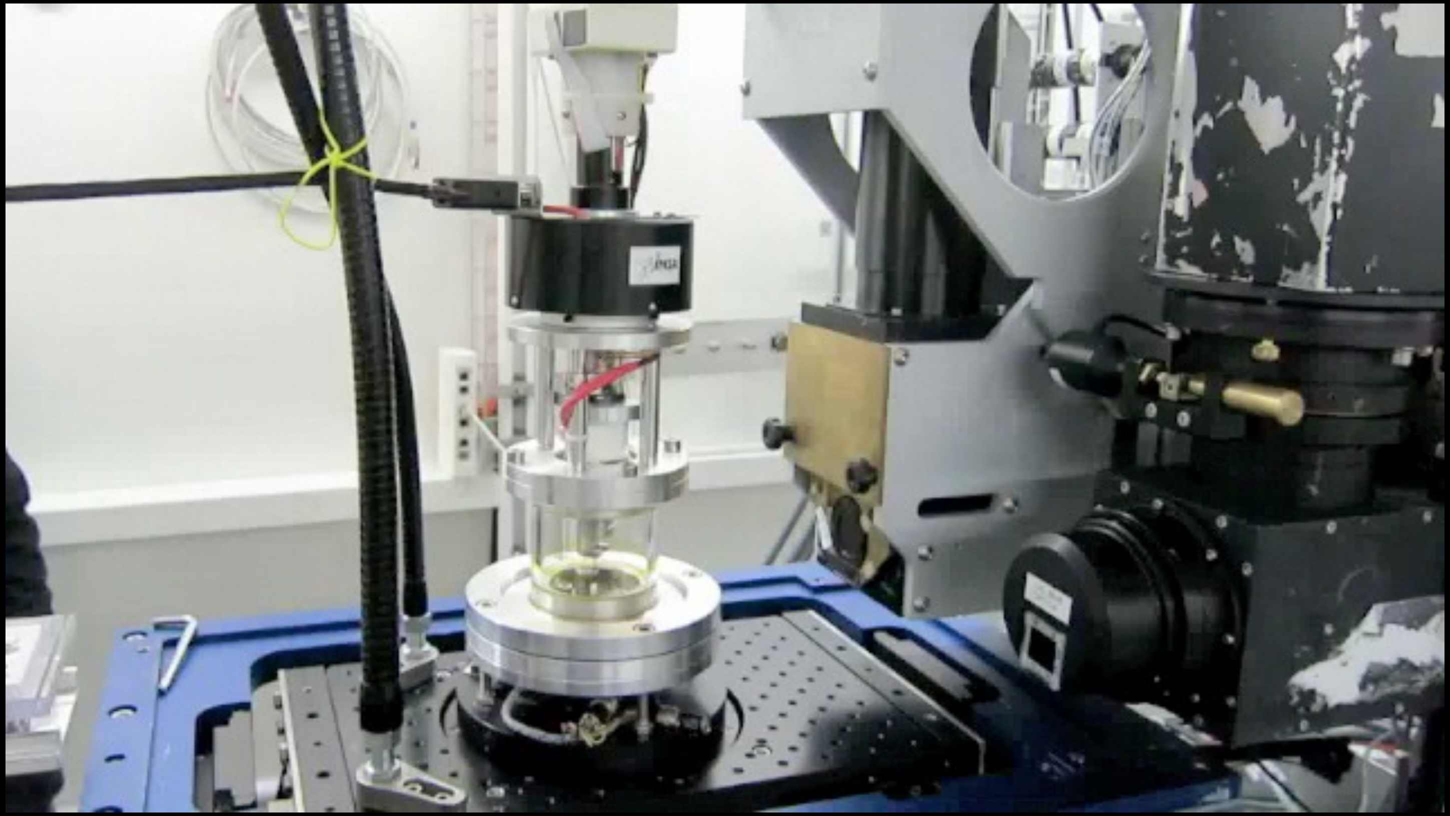

Al - Alumina sample (Eric Maire, Joel Lachambre, INSA Lyon, France)

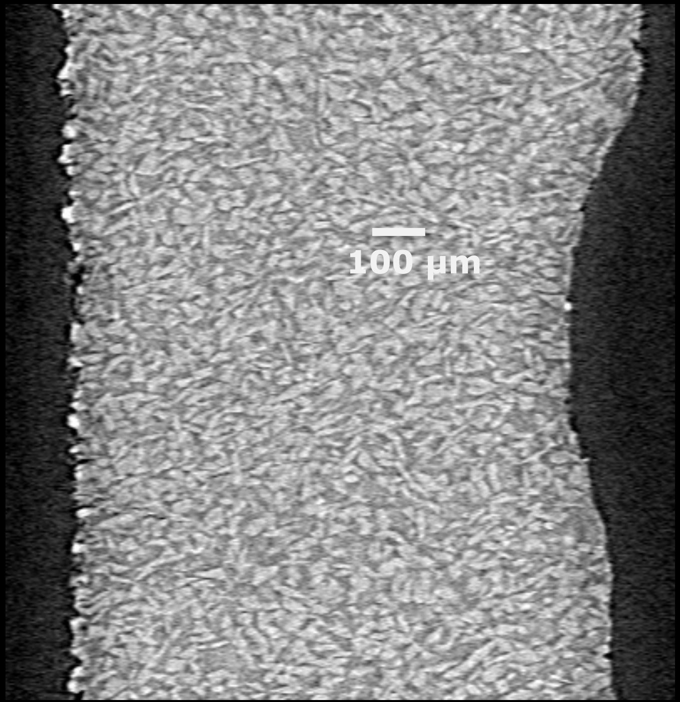

Vertical tomographic slice, time separation ~ 50 ms, voxel = 3μm

E. Maire et al. Int. J. Fraction 2015

Fatique cracking in Alumina sample

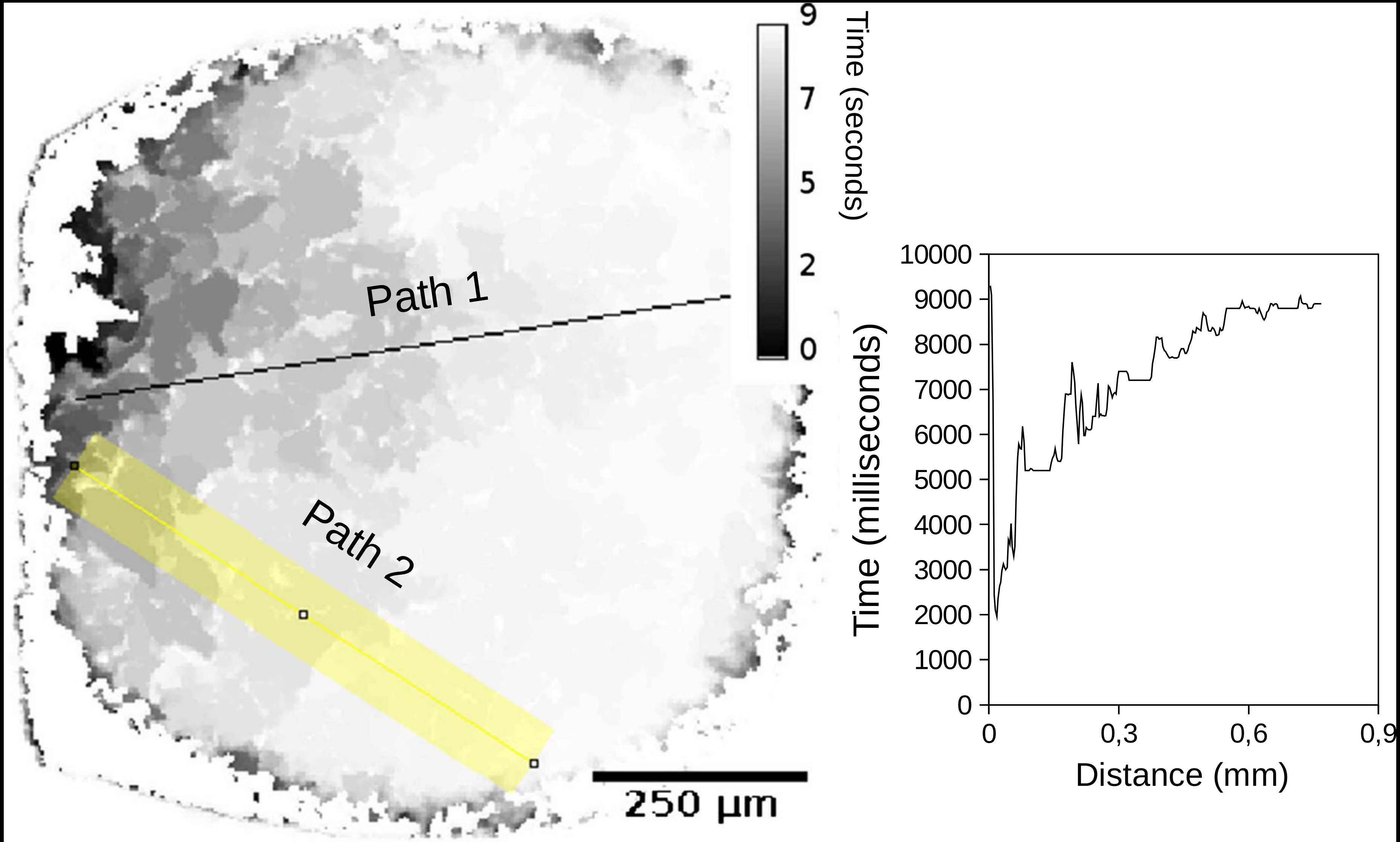

Maire et al., Int J Fracture 2016

Ti-6Al-4 Sintering

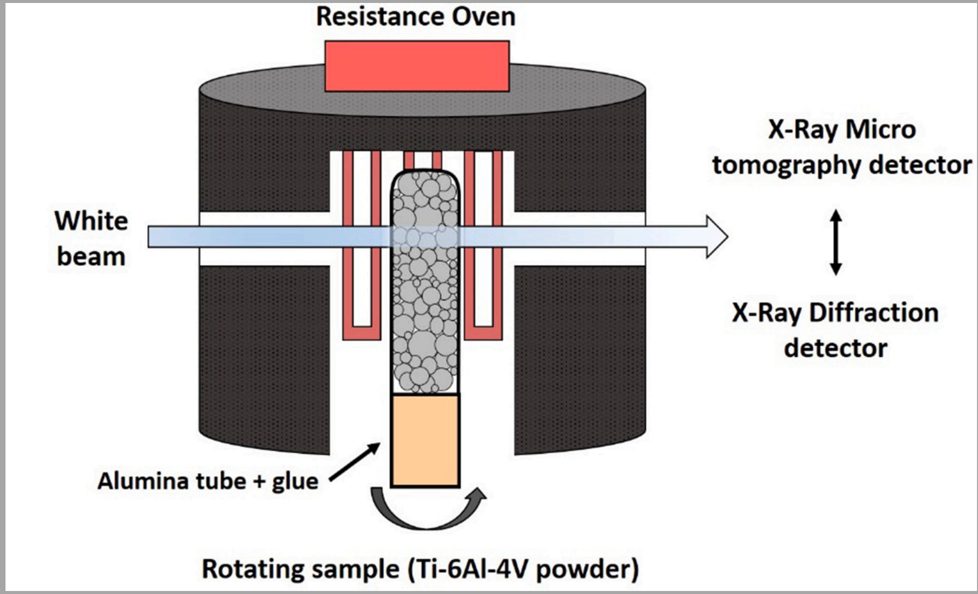

Ti-6Al-4 V gas-atomized powders

ELSEVIER

Acta Materialia

journal homepage: www.elsevier.com/locate/actamat

Full length article

In situ synchrotron study of sintering of gas-atomized Ti-6Al-4 V powder using concomitant micro-tomography and X-ray diffraction: Effect of particle size and interstitials on densification and phase transformation kinetics

M. Pontoreau [a], M. Coffigniez [a], V. Trillaud [a], C. Le Bourlot [a], J. Lachambre [a], L. Gremillard [a], M. Perez [a], E. Maire [a], J. Adrien [a], P. Steyer [a], T. Douillard [a], A. King [b], X. Boulnat [a,*]

[a] *INSA Lyon, University of Lyon, MATEIS, UMR CNRS 5510, F69621 Villeurbanne, France*
[b] *Synchrotron Soleil, Psiché Beamline, F-91190 Gif-sur-Yvette, France*

Ti-6Al-4 Sintering

In-situ tomographic microscopy

Voxel size =650 nm

X-ray energy (pink) ~ 30-80 keV

Acquisition time ~ 6 s

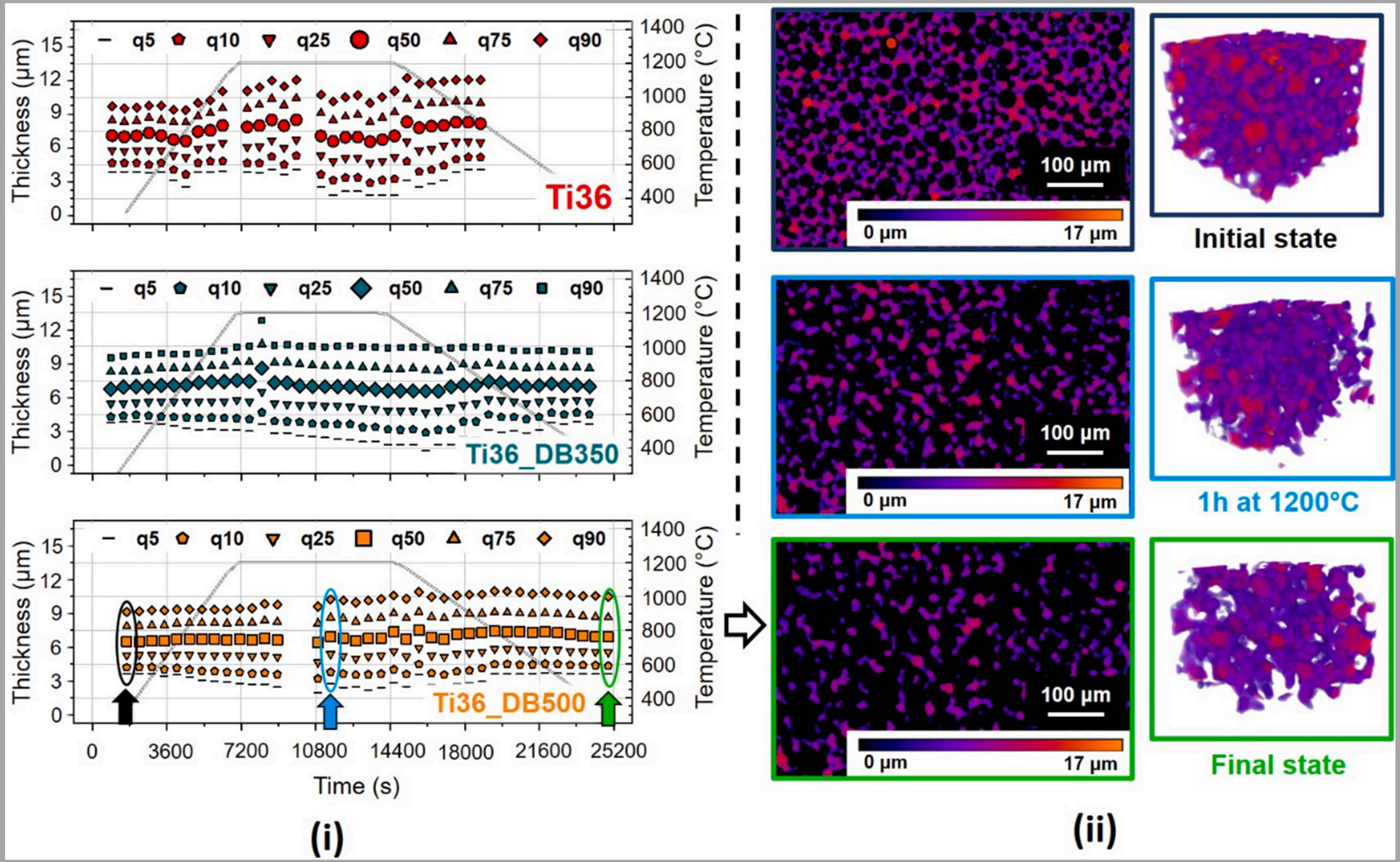

Fig. 4. Interconnected pore evolution for all samples with (i) the evolution of the thickness of their branches and (ii) 2D and 3D (135 × 108 × 133 μm^3) representation of local thickness plugin used on sample Ti36_DB500 (one slice and less than 1 vol% of total 3D volume).

During sintering, the thickness of the interconnected pore is globally stable despite the shrinkage of the interconnected pore network => suggests that the decrease in volume of the interconnected pores network only happens by the closure of the branches composing the interconnected pore rather than an isotropic shrinkage.

Healing in metals

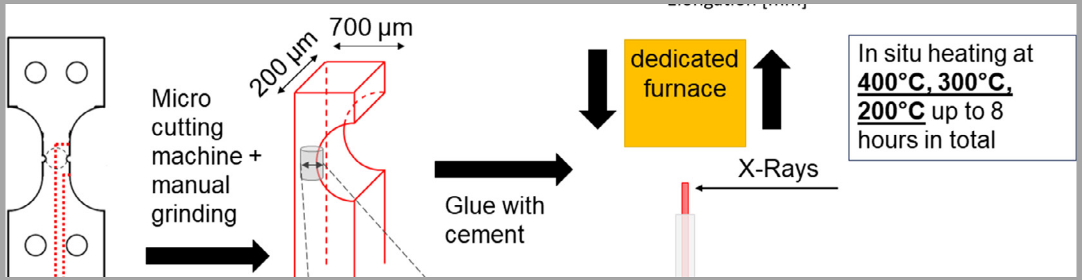

A new precipitation based healing strategy for metals demonstrated on the commercial Al 6063 alloy.

Contents lists available at ScienceDirect

Acta Materialia

journal homepage: www.elsevier.com/locate/actamat

Full length article

A new healing strategy for metals: Programmed damage and repair

Mariia Arseenko[a], Florent Hannard[a], Lipeng Ding[a,b,c], Lv Zhao[a,d], Eric Maire[e], Julie Villanova[f], Hosni Idrissi[a,b], Aude Simar[a,*]

[a] *Institute of Mechanics, Materials and Civil Engineering, UCLouvain, Louvain-la-Neuve 1348, Belgium*
[b] *Electron Microscopy for Materials Science, University of Antwerp, Antwerp 2000, Belgium*
[c] *Key laboratory for Light-Weight Materials, Nanjing Tech University, Nanjing 211816, China*
[d] *Department of Mechanics, School of Aerospace Engineering, Huazhong University of Science and Technology, Wuhan 430074, China*
[e] *Mateis, INSA Lyon, Université de Lyon, Villeurbanne F-69621, France*
[f] *ESRF - The European Synchrotron, Grenoble 38043, France*

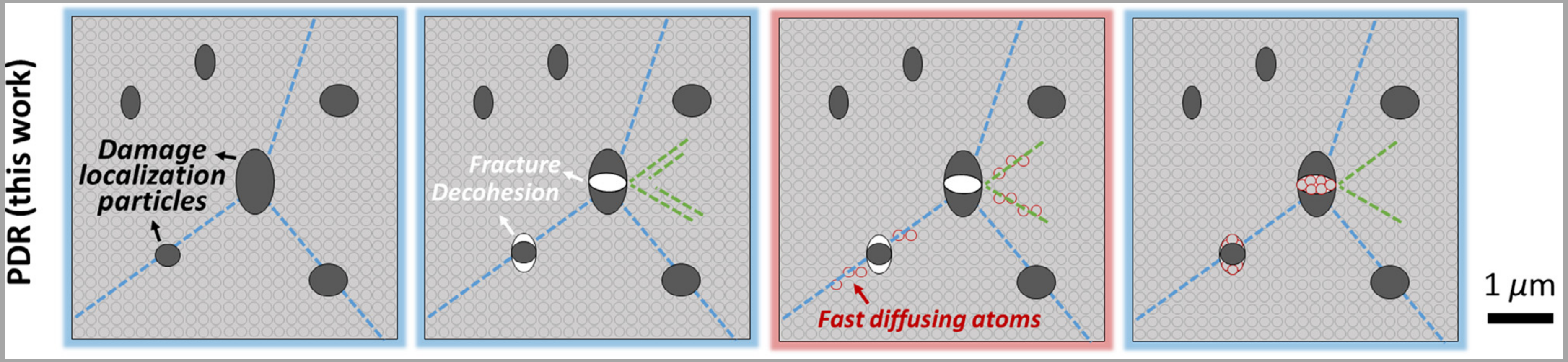

Programmed Damage and Repair

Healing in metals

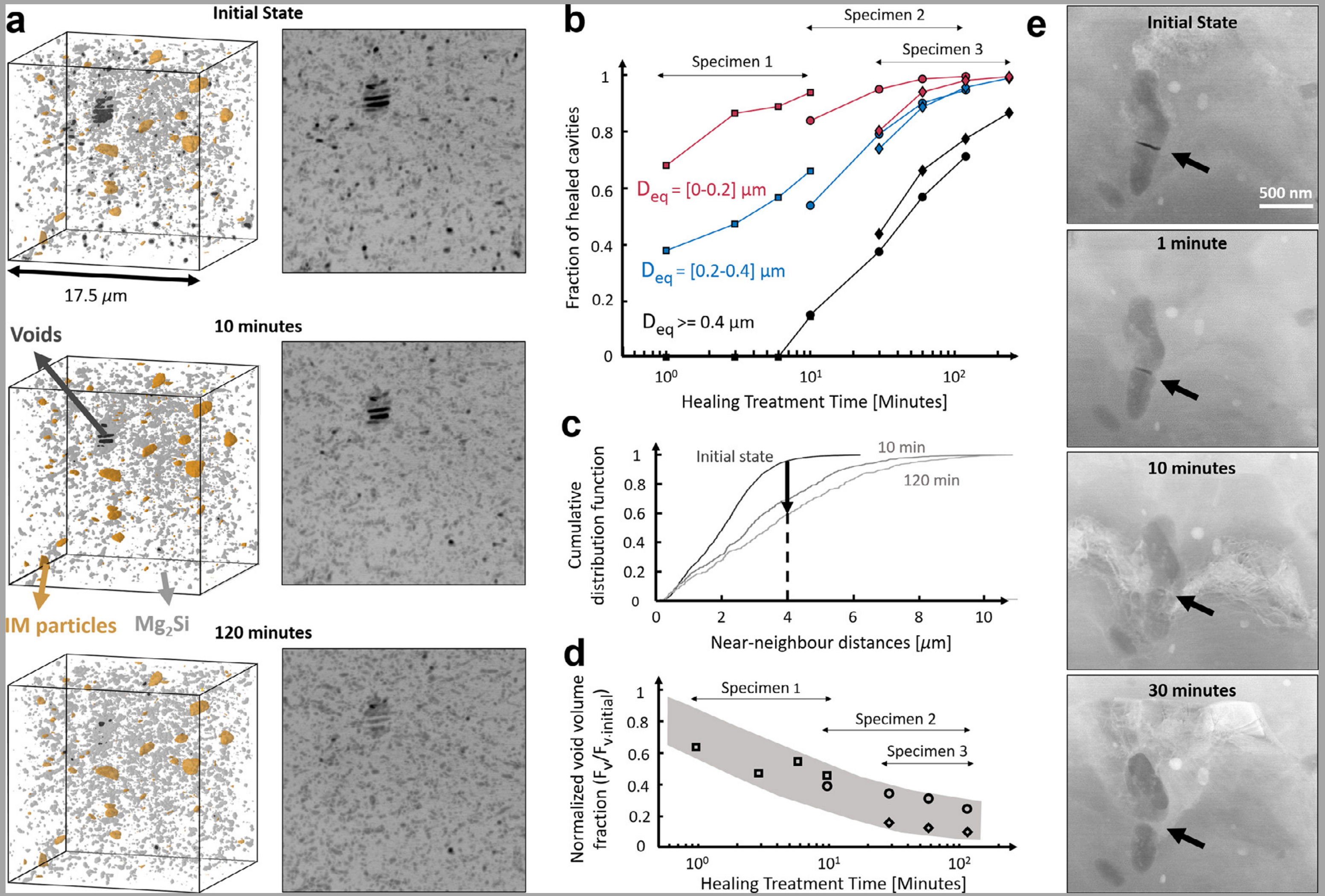

Fig. 6. Healing evolution with time at 400°C. (a) 3D volumes and corresponding Minimum Intensity Projections (MinIP) in the initial state, after 10 min and after 2 h at 400 °C; (voids are in black, intermetallic particles in yellow and Mg_2Si particles in grey). (b) Evolution of the number of healed cavities with healing time for different size classes: Specimens 1 and 2 correspond to 0.6 mm of global elongation; Specimen 3 corresponds to 0.7 mm of global elongation (see Supplementary material 2 for details on each specimen). (c) Cumulative distribution function (CDF) of the near-neighbour distances between voids as a function of the heating time. (d) Evolution of the void volume fraction (F_v), normalised by the value in the initial state ($F_{v,init}$). (e) HAADF-STEM images showing healing evolution with time. The black arrows indicate the position of the crack.

In-situ holotomography with

Voxel size =35 nm

X-ray energy = 17.5 keV

Acquisition time ~ 20 min

Fully exploited coherence properties of the new machines.

Nanoimaging of particles in LiNi type cathode material

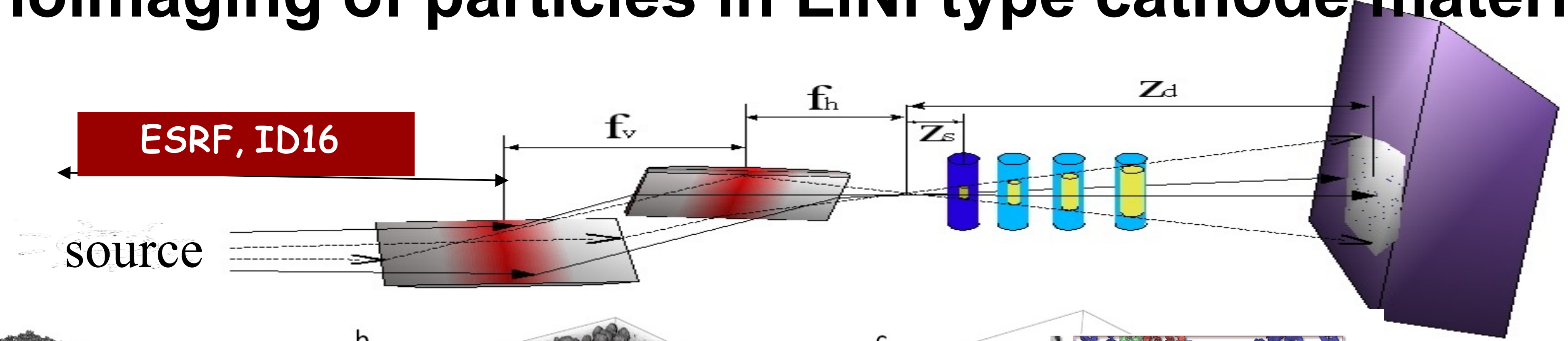

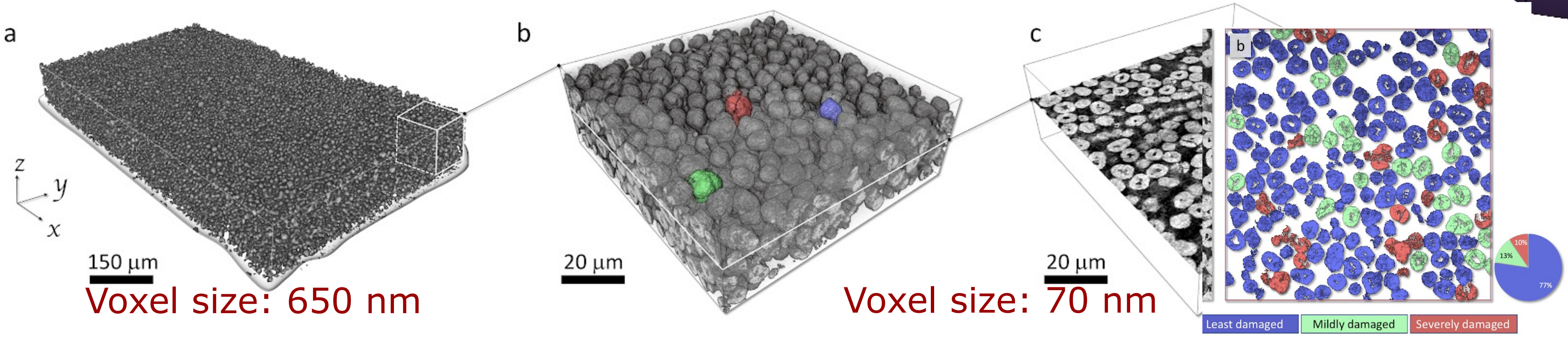

Voxel size: 650 nm

Voxel size: 70 nm

Ni rich cathode material: $LiNi_{1-x-y}Mn_xCo_yO_2$

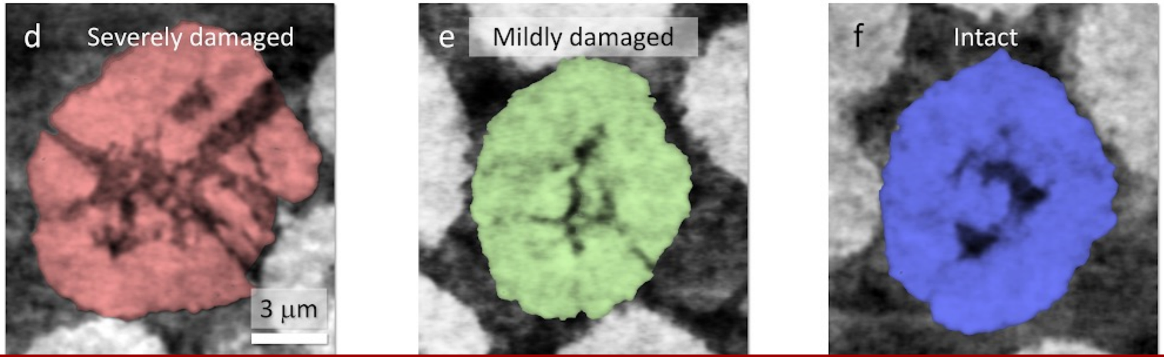

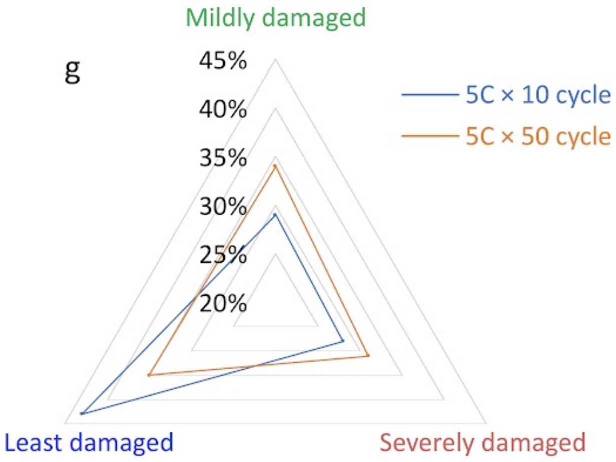

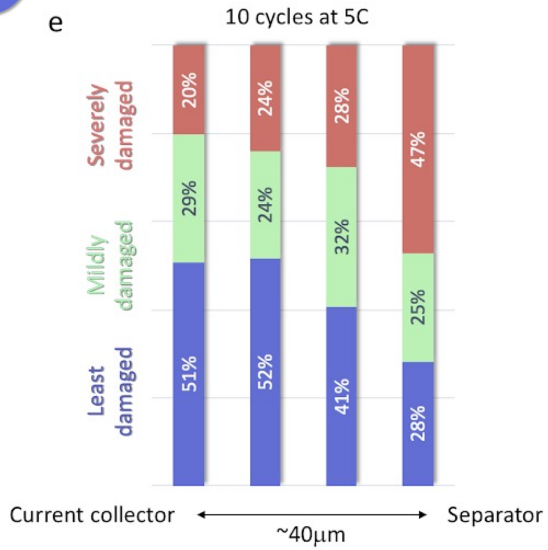

Y. Yang, Y. Liu, et al., Adv. Energy Mater. (2019)

Critical components of success

weak contrast between metallic phases

Optimized phase contrast acquisition and reconstruction

Full exploitation of coherence of the beam

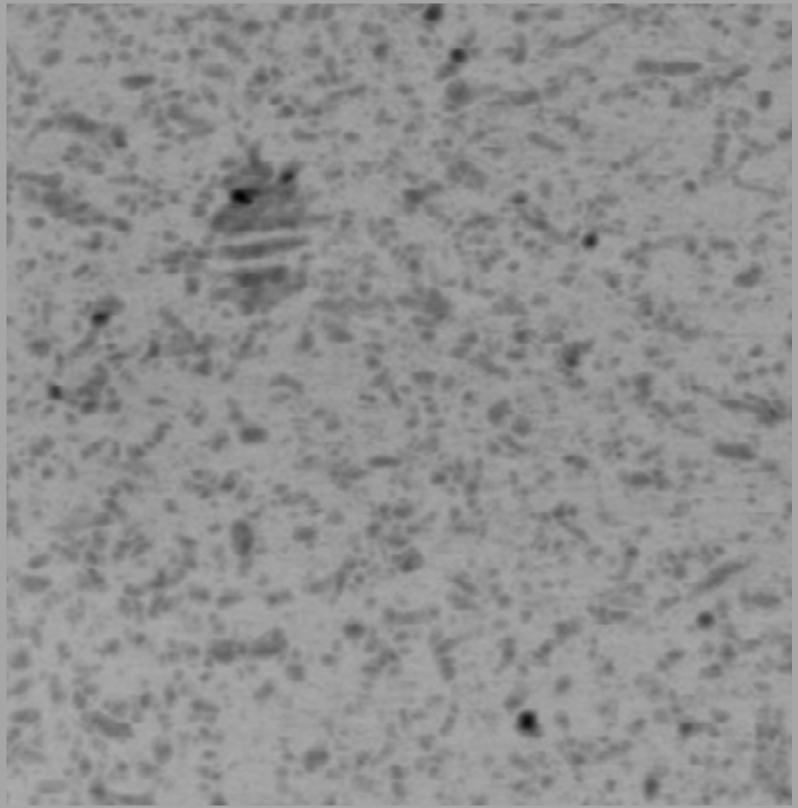

need of reliable and non-manual quantification of fine and complex structures

Artefacts-free reconstructions (avoid rings, gradients, structured noise – local tomo)

Clean X-ray wavefront

As perfect (and as few) beamline optics as possible

Representative volumes

Maximized aspect ration between FOV and resolution

Large beam /detector

Aluminum foams

High speed imaging

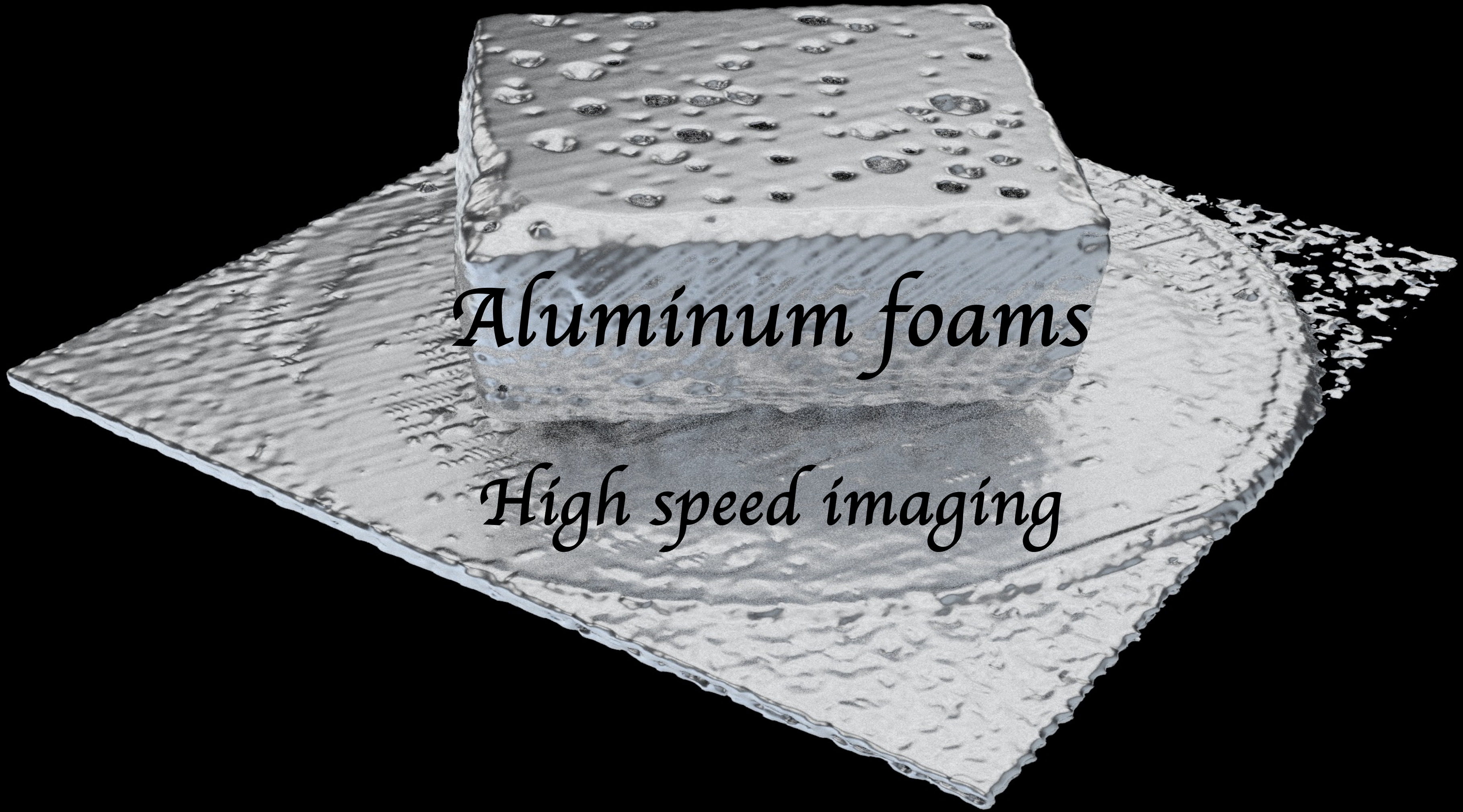

Why Alu?

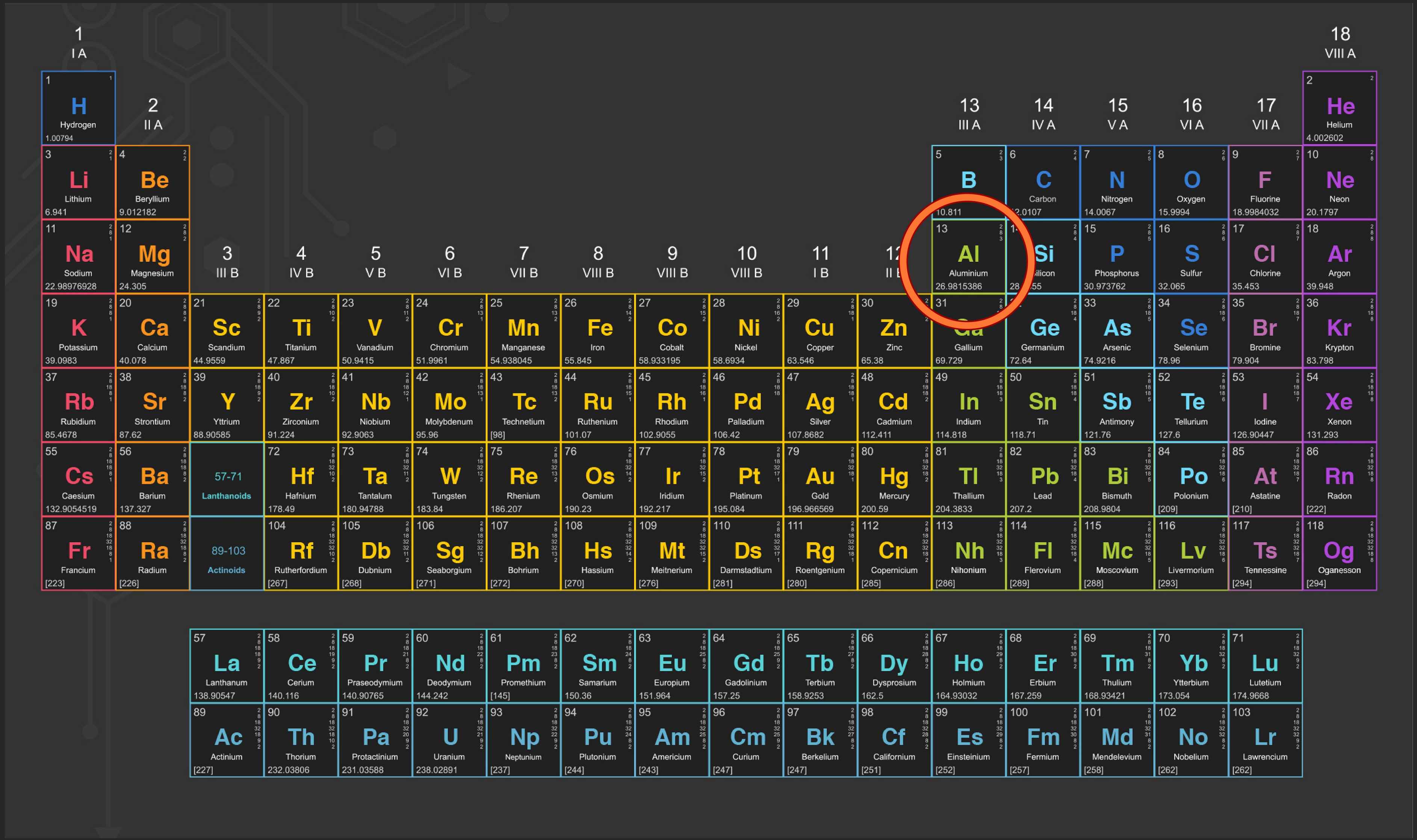

Simplest to image relevant sized samples at a usual imaging beamline at 3rd gen synchrotrons

Nanoparticle stabilization for industrial Al foam production

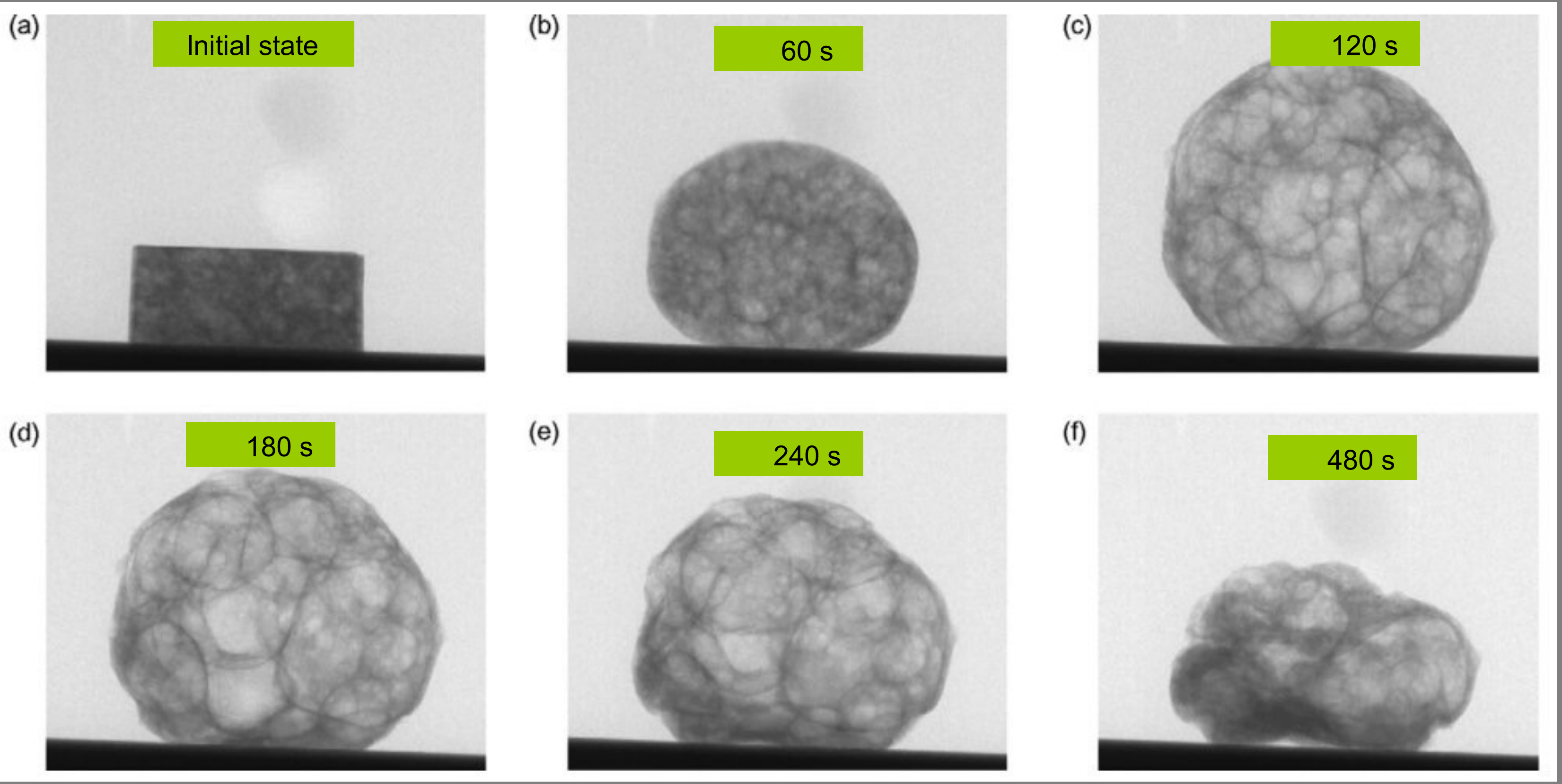

Babcsan, Moreno, Banhart, Colloinds & Surfces A 2007

Precursor made from oxidized melt heated slightly above the melting point.

From materials to devices

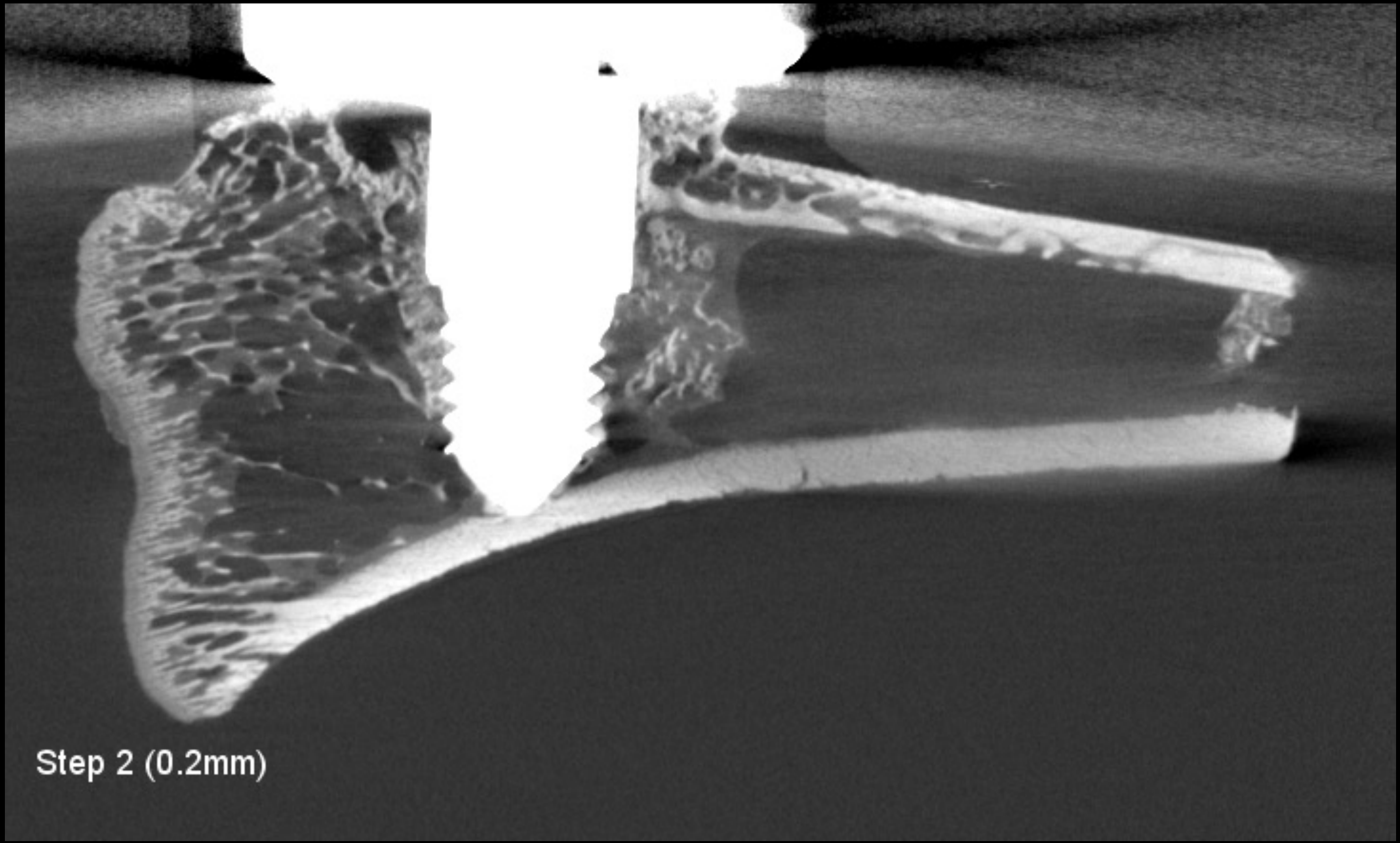

Interfaces between high and low Z materials are difficult

The important contribution of phase contrast at high energies

4D imaging lab,

Zeiss, Solid mechanics, LU

Le Cann et al., Front. Bioeng. Biotechnol 2019

Discussion

I. *Which type of materials are you interested in? (Al, Mg…)*

II. *Any interest in samples with more than 1 mm steel?*

III. *Are large batches of samples relevant? (automation of acquisition)*

IV. *For in-situ studies, do you have your own sample environment? Compatible with X-ray tomo?*